Structure, Vol. 9, 65–71, January, 2001, ©2001 Elsevier Science Ltd. All rights reserved. PII S0969-2126(00)00558-X

Crystal Structure of Phosphoserine Phosphatase from *Methanococcus jannaschii*, a Hyperthermophile, at 1.8 Å Resolution

Weiru Wang,* Rosalind Kim,† Jaru Jancarik,* Hisao Yokota,† and Sung-Hou Kim*†‡
*Department of Chemistry
University of California, Berkeley
Berkeley, California, 94720
†Physical Biosciences Division
Lawrence Berkeley National Laboratory
Berkeley, California 94720

Summary

Background: D-Serine is a co-agonist of the N-methyl-D-aspartate subtype of glutamate receptors, a major neurotransmitter receptor family in mammalian nervous systems. D-Serine is converted from L-serine, 90% of which is the product of the enzyme phosphoserine phosphatase (PSP). PSP from *M. jannaschii* (MJ) shares significant sequence homology with human PSP. PSPs and P-type ATPases are members of the haloacid dehalogenase (HAD)-like hydrolase family, and all members share three conserved sequence motifs. PSP and P-type ATPases utilize a common mechanism that involves Mg^{2+}-dependent phosphorylation and autodephosphorylation at an aspartyl side chain in the active site. The strong resemblance in sequence and mechanism implies structural similarity among these enzymes.

Results: The PSP crystal structure resembles the NAD(P) binding Rossmann fold with a large insertion of a four-helix-bundle domain and a β hairpin. Three known conserved sequence motifs are arranged next to each other in space and outline the active site. A phosphate and a magnesium ion are bound to the active site. The active site is within a closed environment between the core α/β domain and the four-helix-bundle domain.

Conclusions: The crystal structure of MJ PSP was determined at 1.8 Å resolution. Critical residues were assigned based on the active site structure and ligand binding geometry. The PSP structure is in a closed conformation that may resemble the phosphoserine bound state or the state after autodephosphorylation. Compared to a P-type ATPase (Ca^{2+}-ATPase) structure, which is in an open state, this PSP structure appears also to be a good model for the closed conformation of P-type ATPase.

Introduction

The N-methyl-D-aspartate (NMDA) subtype of glutamate receptors belongs to a major neurotransmitter receptor family in mammalian tissues, especially in the nervous system. D-Serine, the co-agonist of the NMDA receptor, is converted from L-serine, 90% of which is the product of the enzyme phosphoserine phosphatase (PSP) [EC 3.1.3.3]. Its enzymatic reaction is Mg^{2+}-dependent and results in the dephosphorylation of phospho-L-serine with the formation of a phosphoenzyme intermediate that is subsequently autodephosphorylated. L-serine is the direct precursor of D-serine [1], and a serine racemase localized in the brain has been shown to racemize L-serine to D-serine [2]. NMDA receptors require coactivation at a glycine site where D-serine, which is present in high levels in mammalian brain, is three times more potent than glycine [3]. Recently, some NMDA receptors have been found to be activated by glycine or D-serine alone in the absence of glutamate [4].

Sequence analysis shows that PSP belongs to the haloacid dehalogenase (HAD) superfamily of hydrolases, which comprises phosphatases, epoxide hydrolases, and L-2-haloacid dehalogenases [5]. Enzymes in this superfamily contain three highly-conserved sequence motifs: motif I: DXDX[T/V][L/V]; motif II: [S/T]XX; and motif III: K-[G/S][D/S]XXX[D/N] (Figure 1). The first Asp in motif I is the residue that gets phosphorylated [6].

The catalytic subunit of P-type ATPases was later included in the HAD superfamily [7] because the same three motifs are present and highly conserved within the P-type ATPases. They share the unique sequence DKTGTL for motif I where the Asp residue is phosphorylated by ATP [8]. Motif III is particularly conserved between PSPs and P-type ATPases (GDGXXD), whereas motif III of HAD adopts a different sequence (SSXXD) [9]. P-type ATPases are essential ion pumps [10]. The ATP hydrolysis requires Mg^{2+} and involves a phosphoryl-aspartyl enzyme intermediate as well as conformational changes that presumably enable transport of ions. Recently, the crystal structure of a member of the P-type ATPase family, calcium ATPase of skeletal muscle sarcoplasmic reticulum, has been solved at 2.6 Å resolution [11] with two calcium ions bound in the transmembrane domain. The phosphorylation domain has the same fold as HAD, and the structure is in an open conformation.

In an effort to understand PSP, a major producer of the precursor of the NMDA receptor co-agonist, we have expressed PSP coded by MJ1594 gene from *Methanococcus jannaschii* (MJ), a hyperthermophile. MJ PSP shares 31% sequence identity and 52% similarity with human PSP (Figure 1). In this work we present the crystal structure of MJ PSP, the third representative of the HAD family, at 1.8 Å resolution.

Results and Discussion

Description of the Structure

The refined PSP structure comprises two molecules (A and B) in each asymmetric unit. The electron density of Asp-11, the phosphorylation site residue, indicated multiple side chain conformations. Therefore, the final

‡To whom correspondence should be addressed (e-mail: shkim@cchem.berkeley.edu).

Key words: haloacid dehalogenase-like hydrolase family; phosphoaspartyl enzyme; phosphoserine phosphatase; Rossman fold

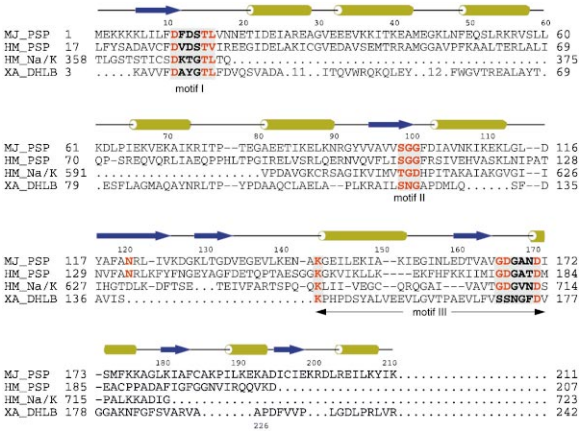

Figure 1. Sequence Comparison of PSP and Its Homologs

Sequence alignment of *M. jannaschii* PSP (MJ_PSP), human PSP (HM_PSP), human Na^+/K^+ pump P-type ATPase (HM_Na/K), and haloacid dehalogenase from *X. autotrophicus* (XA_DHLB). The XA_DHLB sequence is aligned to MJ_PSP based on structure alignment. The "-"s represent gaps and "."s represent regions that cannot be aligned based on current knowledge.

model contains two conformers for this residue. The coordinate error was estimated to be 0.205 Å based on a Luzzati plot [12]. A Ramachandran plot reveals that most of the residues (96.6%) are in the most favored regions, and the remainders are in the additional allowed regions.

The overall monomeric PSP molecule has an oval shape with approximate dimensions of 58 $Å^3 \times$ 35 $Å^3 \times$ 35 $Å^3$. A ribbon diagram and a topology diagram of a monomer Cα trace are shown, respectively, in Figures 2a and 3b. The monomer consists of two domains: a core α/β domain and a four-helix-bundle domain. The core α/β structure displays a six-stranded parallel β-pleated sheet with strands ordered as S3S2S1S5S6S7. This domain resembles an NAD(P) binding Rossmann fold [13] with the addition of a β hairpin located between the third β strand and the third α helix. The carboxyl end of S3 extends out of the core β sheet and, together with S4, forms a β-hairpin. Residue Asn-121, interacting with motif II and located in the β hairpin, is absolutely conserved in the alignment of 19 PSP sequences (data not shown). This suggests that Asn-121 is of structural or catalytic importance.

The four-helix-bundle domain delineates residues 21 to 73, displaying a distorted four-helix-bundle structure comprised of α helices (H1, H2, H3, and H4) that are packed in an approximately antiparallel manner. The helical domain is connected to the core α/β domain via loops 12–20 and 74–80. Loop 12–20 contains the motif I residues and is part of the active site.

The active site is defined by the clustering of the three conserved sequence motifs, and by the bound Mg^{2+} and phosphate in the structure (Figure 2a). As viewed in Figure 2a, the core α/β domain cradles the active site, and the helical domain covers the top. An extensive H bond network connecting the Mg^{2+} ion, the phosphate, and the active site residues is observed (Figure 2b).

Structural Similarity with Other Proteins

The Dali algorithm [14] revealed that the HAD structure is the closest fold homologue to PSP among proteins in PDB. Figures 3a and 3b compare the topology of HAD from *Xanthobacter autotrophicus* (DhlB) and MJ PSP [15]. Both structures contain a modified NAD(P) binding Rossmann fold with a large insertion of a four-helix-bundle subdomain. The two Cα traces can be aligned with each other with an rmsd of 3.75 Å.

PSP is also structurally related to CheY, a response regulator of a two-component signal transduction pathway [16] (Figure 3c). CheY represents a family of response regulators that involve the Mg^{2+}-dependent formation of a phosphoryl-aspartyl enzyme intermediate. Members of this family, including Etr1[17], NtrC [18], Spo0A [19], CheB [20], NarL [21], and FixJ [22] share extensive structural similarity. Remarkably, both PSP and CheY share similar catalytic residues at the active site (Asp-11, Ser-99, Lys-144, and Asp-167 of PSP versus Asp 57, Thr 87, Lys 109, and Asp 13 of CheY), perhaps due to a similar reaction mechanism (Figure 3d). After superimposing the two active sites, we obtained a good alignment of the overall structure of CheY to the α/β domain of PSP with an rmsd of 1.4 Å. Interestingly, the active site guided structural alignment reveals a circular permutation between the topology of PSP and CheY. CheY adopts the 2–1-3–4-5 topology of a parallel β sheet as shown in Figure 3c. A circular permutation of CheY, made by joining the N- and C- termini while cutting between H2 and S3, would convert CheY to the PSP α/β domain topology 3–2-1–4-5(-6) with retention of the active site configuration and overall structure.

Implications for Enzymatic Mechanism

PSP activity has an absolute requirement for Mg^{2+} ion (data not shown), which is found directly coordinated with Asp-11 and phosphate in the structure (Figure 2b). Conformer 1 of Asp-11 may resemble the conformation of phosphoserine-bound state or the state after autodephosphorylation because, in this orientation, one of the Asp-11 oxygens (Oδ1) is close (2.90 Å) to the phosphorus atom. This oxygen atom is likely to perform the nucleophilic attack to the phosphorous atom. Asp-167 is a key coordinator to the Mg^{2+} ion. In fact, mutation of Asp-167 to Glu or Asn resulted in a dramatic loss of affinity to Mg^{2+} in the human enzyme [23]. The direct coordination of phosphate with Mg^{2+} may polarize the P-O bond and increase the electrophilicity of the phosphorus atom as proposed previously [24]. The interaction of four amide groups (D13, S14, G100, and N170) and the side chains of Ser-99 and Lys-144 with the phosphate oxygens (Figure 2b) could also increase the electrophilicity of the phosphorus atom to facilitate the nucleophilic attack on phosphate by D11 and the breakage of the scissile P-O bond of P-L-serine. We propose that the trigonal bipyramid transition state of the phosphate group is stabilized by most of the H bonds that were activating the phosphate group of P-L-serine. Lys-144 is within H bond distance from Asp-11, and may stabilize the negative charge associated with the Asp-11 side chain during the reaction.

We identified the most likely region for binding of the

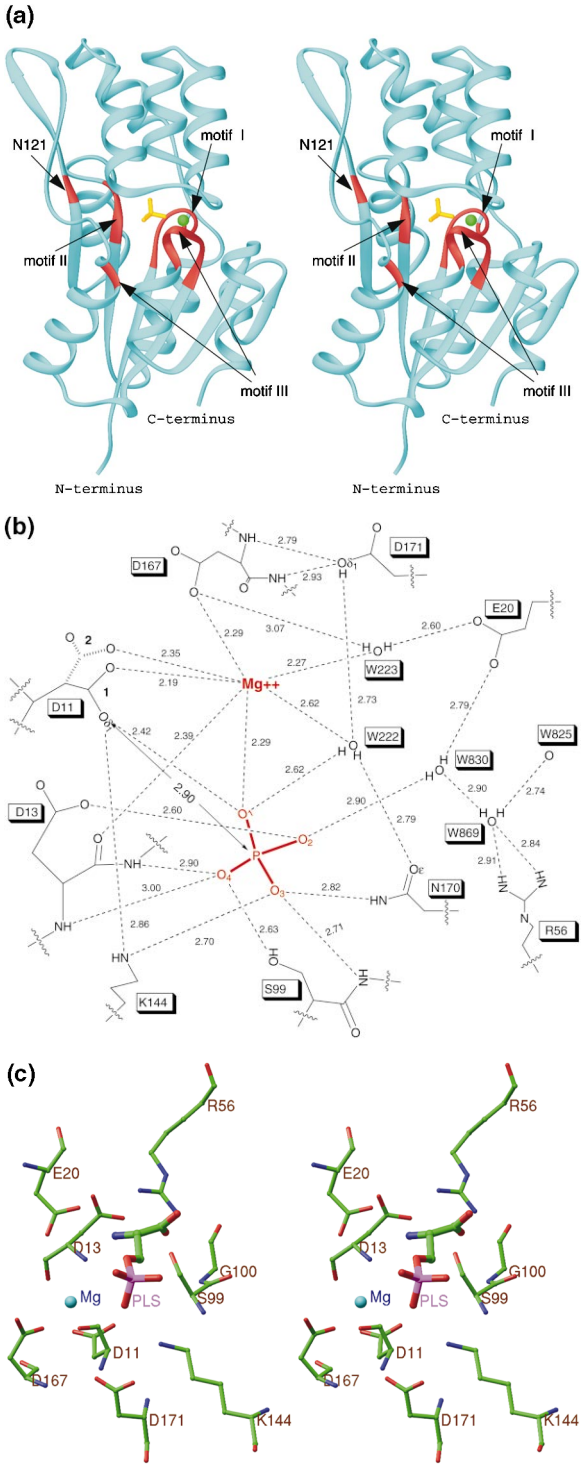

Figure 2. Ribbon Diagram of PSP Structure and Hydrogen Bond Network of Its Active Site

(a) Stereo view of the PSP structure presented in a ribbon diagram. The three conserved motifs are colored in red. The orange molecule depicts the phosphate in the active site. The green ball depicts the Mg^{2+} ion.

(b) A schematic plot of the hydrogen bond network in the active site. All the H bonds that involve the ligands, and part of the H-bonds that do not involve the ligands, are shown as dotted lines. The unit for the distances is in Å. The Mg^{2+} achieves the hexavalent coordination through interactions with the phosphate, Asp-11, Asp-13, Asp-167, and water molecules W222 and W223. W222 and W223, in turn, interact with the surrounding residues including Asp-167, Glu-20, Asp-171, Asp-170, and the phosphate. Asp-11 adopts discrete sidechain conformations 1 and 2. Both conformations coordinate with the Mg^{2+}. Conformer 1 also interacts with the phosphate while conformer 2 is remote form the phosphate but forms an H bond with the Thr-15 sidechain. The phosphate forms H bonds with residues from all three motifs. The H bond between O1 and Asp-11 suggests that either O1 or Asp-11 is protonated. Similarly, either O2 or Asp 13 has to contribute a proton to achieve the H bond between them.

(c) Active site residues of PSP and the theoretical model of its substrate, P-L-serine.

serine group of the substrate within the current structure (Figure 2c). We modeled the substrate-bound structure by attaching serine to the phosphate-bound structure while maximizing H bond interactions. This region, immediately adjacent to the phosphate, is occupied by four water molecules (W869, W830, W826 and W825), and located at the interface between the α/β domain and the four-helix-bundle domain. The two domains come together and form a pocket that is composed of the side chains of Asp-13, Glu-20, Thr-39, Met-43, Phe-49, Arg-56, and Asn-170, and the backbone of Gly-100 and Gly-101. Specificity and orientation of the substrate may be facilitated by part of this pocket surface. Model building suggests that a serine residue can very convincingly replace the space occupied by these water molecules making the same hydrogen bonds. The sidechains of Asp-13 and Asn-170 and the mainchain amide of Gly-100 are located in close proximity of phosphoserine. They may contribute to stabilizing the oxyanion carried by the leaving group during the reaction. Asp-13 belongs to motif I and is conserved as D/E among nineteen PSPs. Our structure shows that Asp-13 forms two H bonds: one as an H bond acceptor from the amide group of Thr-21 and the other as an H bond donor to a Pi oxygen. These interactions indicate that Asp-13 is in a protonated state. Asn-170 belongs to motif III and is conserved as N/T among 18 out of 19 PSPs. These may be interesting targets for mutagenesis studies.

Previous mechanism studies based on human PSP showed that mutations of residues S99A, K144A/R, D167N, and D171N significantly lower PSP activity [23]. Our structure reveals that S99 and K144 form hydrogen bonds with the phosphate. D167 forms a coordination bond to Mg^{2+} and D171 stabilizes motif III that forms the Mg^{2+} binding loop.

In the current PSP structure, the active site is within a closed environment between the core α/β domain and the four-helix-bundle domain. In fact, the PSP active site is buried under the molecular surface (Figure 4), suggesting that the enzymatic reaction involves some type of conformational rearrangement that enables access of substrate and the release of products. Scarborough [25] proposed that P-type ATPases possess an open conformation in the absence of ligand and a closed conformation upon enzyme phosphorylation. The catalytic reactions lead to repeating cycles of conformational oscillation. Given the homology in sequence and similarity in enzyme mechanism between PSP and the phosphorylation domain of P-type ATPase, their dynamics may

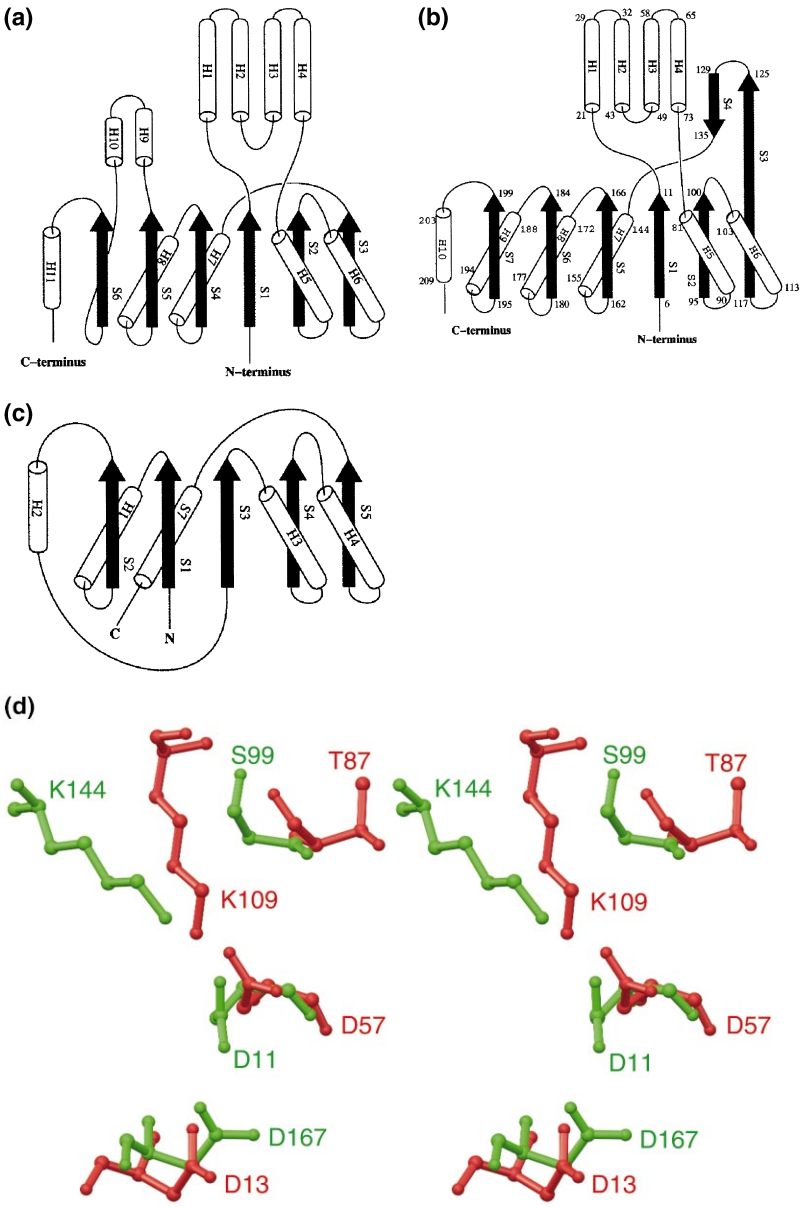

Figure 3. Topology Diagram of Three HAD Family Representatives

(a) Haloacid dehalogenase from *X. autotrophicum*; (b) MJ PSP; (c) *E. coli* CheY. Haloacid dehalogenase and PSP share identical topology except that PSP has an extra β-hairpin insertion, whereas DhlB contains an extra small helical structure extending out of the core β sheet. Compared to MJ PSP, CheY possesses an α/β domain with five β strands and five helices, but is missing the helical bundle, the β hairpin, and S7, H9 of PSP; (d) Stereo view of the active site of PSP (green) superimposed on that of CheY (red).

also be related. The crystal structure of Ca^{2+}-ATPase is in an open state, where the phosphorylation site is more than 25 Å away from the presumed ATP binding site [11]. The current PSP structure is in a closed conformation, and may be a good model for the closed conformation of P-type ATPase.

Biological Implications

PSP exists in high abundance in mammalian brain. Its product, L-serine, is a precursor for the biosynthesis of glycine. Thus PSP may also regulate the levels of glycine and D-serine, the putative co-agonists for the glycine site of the NMDA receptor in brain. It has been observed that D-serine is more potent than glycine in activating the NMDA receptor [3, 26]. Until recently, when a mammalian serine racemase was identified in rat brain [2], the formation of D-serine by serine racemase had been identified only from bacterial sources and insects. Stimulation of NMDA receptors after a stroke, due to a massive release of glutamate, is thought to be responsible for a large portion of neural damage; and drugs that block the glycine site of NMDA receptors prevent stroke damage [27, 28]. It may be possible to regulate NMDA activity by using selective inhibitors against serine racemase and/or PSP. The structural information of PSP should provide a structural basis for designing inhibitors of this enzyme, which may modulate D-serine levels in the brain.

PSP has significant sequence homology and striking similarity in enzyme mechanism with the phosphorylation domain of P-type ATPases. A thorough understanding of the PSP reaction mechanism based on the high-resolution structure may also provide important information for the mechanistic studies of P-type ATPase. The atomic resolution crystal structure of Ca^{2+}-ATPase

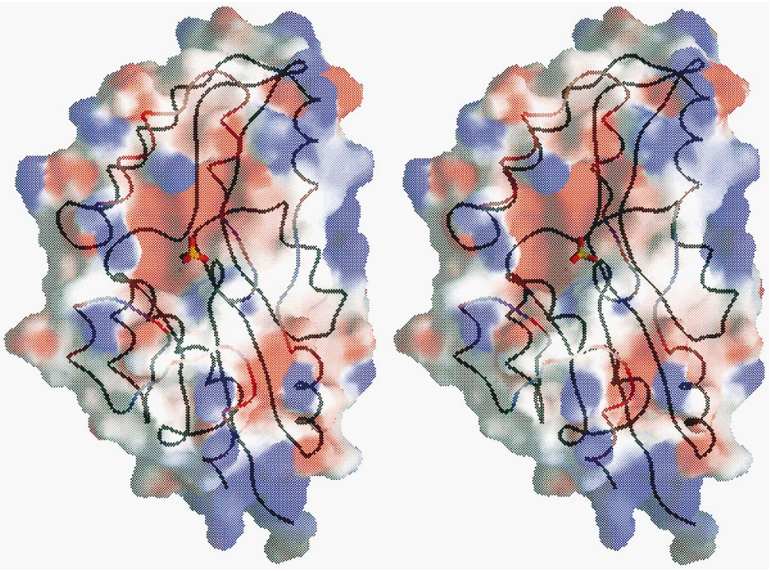

Figure 4. Molecular Surface Colored by Electrostatic Potential

The electrostatic potential and the molecular surface were calculated using only the protein atoms. The ribbon diagram represents the Cα trace. The ball-and-sticks depict the phosphate and Mg^{2+}.

shows it to be in an open state whereas the structure of PSP is in a closed conformation, making the latter a good model for the closed conformation of P-type ATPases.

Experimental Procedures

Cloning, Expression, and Purification

The gene for PSP, MJ1594, was amplified from genomic *M. jannaschii* DNA, cloned into pET21a (Novagen, Madison, WI) and expressed in B834(DE3)/pSJS1244 *E. coli* cells [29] upon induction with 0.5 mM isopropyl-β-d-thiogalactopyranoside. Selenomethionyl (Se-Met) protein was prepared according to the method of Doublie [30]. Frozen cells (8 g) were suspended in 10 ml of 50 mM Tris-HCl (pH 7.5)/25% sucrose, sonicated, and centrifuged at 12,000 × g for 20 min in a Sorvall centrifuge. To remove *E. coli* proteins, the supernatant was heated at 70°C for 20 min and spun in a Beckman ultracentrifuge Ti45 rotor at 70,000 × g for 30 min at 4°C. The heated supernatant was applied onto a Poros HQ/M (PE Biosystems, MA, USA) column equilibrated with 20 mM Tris Bis-Tris Propane (pH 8.3) 10 mm DTT buffer. PSP came out in the flow through. Fractions were pooled, concentrated, and applied onto a 1.5 × 90 cm Sephacryl S-200 HR (Pharmacia, NJ, USA) filtration column that had been equilibrated with 20 mM Tris-HCl (pH 7.5), 0.3 M NaCl, 1 mM EDTA, and 10 mM DTT (Buffer A).

Crystallization

The purity of the expressed PSP was determined by SDS gel electrophoresis and electrospray mass spectrometry. The protein was concentrated in Buffer A to 54 mg ml^{-1}. Crystallization conditions were tested with a sparse matrix sampling method [31], using hanging drop vapor diffusion method with Hampton screen solutions (Hampton Research, CA, USA) at room temperature. The optimum conditions were in 0.1 M sodium acetate buffer (pH 4.5), 0.5 M sodium phosphate dihydrate, and 22% polyethylene glycol 2000 monomethylether (PEG2K MME). Microseeding was performed 1 hr after the drop was set up. Crystals appeared within 12 hr and reached a maximum size of 0.2 × 0.3 × 0.5 mm^3.

Structure Solution and Refinement

X-ray data statistics are shown in Table 1. The Se atom positions were located using SOLVE [32]. Four Se sites were found with a figure of merit (FOM) of 0.69. Phases were subject to 10 cycles of solvent flattening [33] and followed by NCS averaging. Additional NCS partner sites were visually located in a solvent flattened map. An improper 2-fold NCS matrix was determined. The FOM after NCS averaging achieved 0.942 overall and 0.856 in the 2.0 Å resolution shell.

The model building was performed using O [34]. The initial model was traced in the 2.0 Å NCS averaged experimental map for a monomer. A model containing 419 residues was derived from pro-

Table 1. Statistics of X-ray Diffraction Data and Structure Refinement

Data set	Edge	Peak	Remote
Wavelength (Å)	0.979962	0.979725	0.911649
Resolution (Å)	30.0–2.0	30.0–2.0	30.0–1.8
Redundancy	3.6 (3.5)[a]	3.5 (3.6)	3.3 (3.5)
Unique reflections	55,951 (2,245)	55,408 (2,160)	71,908 (2,219)
Completeness (%)	98.6 (88.9)	98.1 (87.3)	95.4 (78.2)
I/σ	30.3 (11.1)	28.8 (10.4)	22.4 (3.5)
R_{sym}[b] (%)	4.4 (12.8)	4.5 (13.3)	5.3 (30.5)

[a] Numbers in parentheses are related to the highest resolution shell, which is 2.03–2.00 Å for edge and peak wavelength data, and 1.83–1.80 Å for remote wavelength data.

[b] $R_{sym} = \Sigma_{hkl}\Sigma_i|I_{hkl,\,i} - \langle I\rangle_{hkl}|/\Sigma|\langle I\rangle_{hkl}|$

The three wavelength MAD data sets were collected at the Stanford Synchrotron Radiation Laboratory (SSRL) beamline 1–5. For this data collection, an Area Detector System Co. (ADSC) Quantum 4 CCD detector was placed 170 mm from the sample. The MAD data were processed with the programs DENZO and SCALEPACK [36].

Table 2. Crystal Parameters and Refinement Statistics

Space group	$P2_12_12$
Cell dimensions	a = 69.0 Å, b = 70.0 Å, c = 91.2 Å
Volume fraction of protein	53%
V_m (Å^3/dalton)	2.33
Total number residues	419
Total non-H atoms	3,707
Number of water molecules	383
Number of phosphate molecules	4
Number of Mg^{2+}	2
Temperature factors	
Protein	15.6 Å^2
Solvent	28.1 Å^2
Metal	16.2 Å^2
Phosphate	16.1 Å^2
Resolution range of reflections used	15–1.8 Å
Amplitude cutoff	No
R factor	19.7%
Free R factor	23.5%
Stereochemical ideality	
Bond	0.018 Å
Angle	1.85°
Improper	1.25°

The remote data set was used for structure refinement.

gressive improvement of the electron density map using rounds of phase combination and manual building.

The preliminary model was then refined against the remote data set to 1.8 Å using CNS [35]. The NCS constraints and restraints were completely released during the refinement. Ten percent of the data were randomly picked out for free R factor cross validation. The refinement statistics are shown in Table 2.

Acknowledgments

We thank Dr. David King for performing the electrospray mass spectrometry, Dr. Henry Bellamy for assistance during data collection, Huy Nguyen for technical support, and Dr. Chao Zhang and Dr. Ho Cho for their helpful discussions. This work was supported by the Director, Office of Science, Office of Biological and Environmental Research, under the U. S. Department of Energy, under Contract No. DE-AC03-76SF00098 (R. K. and S.-H. K.).

Received: July 18, 2000
Revised: November 2, 2000
Accepted: November 2, 2000

References

1. Dunlop, D.S., and Neidle, A. (1997). The origin and turnover of D-serine in brain. Biochem. Biophys. Res. Commun *235*, 26–30.
2. Wolosker, H., et al., and Snyder, S.O. (1999). Purification of serine racemase: biosynthesis of the neuromodulator D-serine. Proc. Natl. Acad. Sci. USA *96*, 721–725.
3. Matsui, T., Sekiguchi, M., Hashimoto, A., Tomita, U., Nishikawa, T., and Wada, K. (1995). Functional comparison of D-serine and glycine in rodents: the effect on cloned NMDA receptors and the extracellular concentration. J. Neurochem. *65*, 454–458.
4. Paudice, P., Gemignani, A., and Raiteri, M. (1998). Evidence for functional native NMDA receptors activated by glycine or D-serine alone in the absence of glutamatergic coagonist. Eur. J. Neurosci. *10*, 2934–2944.
5. Koonin, E.V., and Tatusov, R.L. (1994). Computer analysis of bacterial haloacid dehalogenases defines a large superfamily of hydrolases with diverse specificity. Application of an iterative approach to database search. J. Mol. Biol. *244*, 125–132.
6. Collet, J.-F., Stroobant, V., Pirard, M., Delpierre, G., and Van Schaftingen, E. (1998). A new class of phosphotransferases phosphorylated on an aspartate residue in an amino-terminal DXDX(T/V) motif. J. Biol. Chem. *273*, 14107–14112.
7. Collet, J.-F., Gerin, I., Rider, M.H., Veiga-da-Cunha, M., and Van Schaftingen, E. (1997). Human L-3-phosphoserine phosphatase: sequence, expression and evidence for a phosphoenzyme intermediate. FEBS Lett. *408*, 281–284.
8. Liu, J.Q., Kurihara, T., Miyagi, M., Esaki, N., and Soda, K. (1995). Reaction mechanism of L-2-haloacid dehalogenase of *Pseudomonas* sp. YL. Identification of Asp10 as the active site nucleophile by 18O incorporation experiments. J. Biol. Chem. *270*, 18309–18312.
9. Aravind, L., Galperin, M.Y., and Koonin, E.V. (1998). The HD domain defines a new superfamily of metal-dependent phosphohydrolases. Trends Biochem. Sci. *23*, 127–129.
10. Lingrel, J.B., and Kuntzweiler, T. (1994). Na^+, K^+-ATPase. J. Biol. Chem. *269*, 19659–19662.
11. Toyoshima, C., Nakasako, M., Nomura, H., and Ogawa, H. (2000). Crystal structure of the calcium pump of sarcoplasmic reticulum at 2.6 Å resolution. Nature *405*, 647–655.
12. Luzzati, V. (1952). Remarks about protein structure precision. Acta Cryst. *5*, 802–810.
13. Rossmann, M.G., Moras, D., and Olsen, K.W. (1974). Chemical and biological evolution of nucleotide-binding protein. Nature *250*, 194–199.
14. Holm, L., and Sander, C. (1993). Protein structure comparison by alignment of distance matrices. J. Mol. Biol. *233*, 123–138.
15. Ridder, I.S., and Dijkstra, B.W. (1999). Identification of the Mg^{2+}-binding site in the P-type ATPase and phosphatase members of the HAD (haloacid dehalogenase) superfamily by structural similarity to the response regulator protein CheY. Biochem. J. *339*, 223–226.
16. Stock, A.M., Mottonen, J.M., Stock, J.B., and Schutt, C.E. (1990). Three-dimensional structure of CheY, the response regulator of bacterial chemotaxis. Nature *337*, 745–749.
17. Muller-Dieckmann, H.J., Grantz, A., and Kim, S.-H. (1999). The structure of the signal receiver domain of the *Arabidopsis thaliana* ethylene receptor ETR1. Structure Fold Des. *7*, 1547–1556.
18. Volkman, B.F., Nohaile, M.J., Amy, N.K., Kustu, S., and Wemmer, D.E. (1995). Three-dimensional solution structure of the N-terminal receiver domain of NTRC. Biochemistry *34*, 1413–1424.
19. Lewis, R.J., Brannigan, J.A., Muchova, K., Barak, I., and Wilkinson, A.J. (1999). Phosphorylated aspartate in the structure of a response regulator protein. J. Mol. Biol. *294*, 9–15.
20. Djordjevic, S., Goudreau, P.N., Xu, Q., Stock, A.M., and West, A.H. (1998). Structural basis for methylesterase CheB regulation by a phosphorylation-activated domain. Proc. Natl. Acad. Sci. USA *95*, 1381–1386.
21. Baikalov, I., Schroder, I., Kaczor-Grzeskowiak, M., Grzeskowiak, K., Gunsalus, R.P., and Dickerson, R.E. (1996). Structure of the *Escherichia coli* response regulator NarL. Biochemistry *35*, 11053–11061.
22. Gouet, P., et al., and Samama, J.P. (1999). Structural transitions in the FixJ receiver domain. Structure Fold Des. *7*, 1517–1526.
23. Collet, J.-F., Stroobant, V., and Van Schaftingen, E. (1999). Mechanistic studies of phosphoserine phosphatase, an enzyme related to P-type ATPases. J. Biol. Chem. *274*, 33985–33990.
24. Ridder, I.S., Rozeboom, H.J., Kalk, K.H., Janssen, D.B., and Dijkstra, B.W. (1997). Three-dimensional structure of L-2-haloacid dehalogenase from *Xanthobacter autotrophicus* GJ10 complexed with the substrate-analogue formate. J. Biol. Chem. *272*, 33015–33022.
25. Scarborough, G.A. (2000). Crystallization, structure and dynamics of the proton-translocating P-type ATPase. J. Exp. Biol *203*, 147–154.
26. Berger, A.J., Dieudonne, S., and Ascher, P. (1998). Glycine uptake governs glycine site occupancy at NMDA receptors of excitatory synapses. J. Neurophysiol. *80*, 3336–3340.
27. Choi, D.W., and Rothman, S.M. (1990). The role of glutamate neurotoxicity in hypoxic-ischemic neuronal death. Annu. Rev. Neurosci. *13*, 171–182.
28. Gill, R., Hargreaves, R.J., and Kemp, J.A. (1995). The neuroprotective effect of the glycine site antagonist 3R-(+)-cis-4-methyl-

HA966 (L-687,414) in a rat model of focal ischaemia. J. Cereb. Blood Flow Metab. *15*, 197–204.
29. Kim, R., Sandler, S.J., Goldman, S., Yokota, H., Clark, A.J., and Kim, S.-H. (1998). Overexpression of archaeal proteins in *Escherichia coli*. Biotech. Lett. *20*, 207–210.
30. Doublie, S. (1997). Preparation of selenomethionyl proteins for phase determination. Methods Enzymol. *276*, 523–529.
31. Jancarik, J., and Kim, S.-H. (1991). Sparse matrix sampling: A screening method for crystallization of proteins. J. Appl. Crystallogr. *24*, 409–411.
32. Terwilliger, T.C., Kim, S.-H., and Eisenberg, D. (1987). Generalized method of determining heavy-atom positions using the difference Patterson function. Acta. Crystallogr. *A43*, 1–5.
33. Wang, B.-C. (1985). Resolution of phase ambiguity in macromolecular crystallography. Methods Enzymol. *115*, 90–112.
34. Jones, T.A., Zou, J.-Y., Cowan, S.W., and Kjeldgaard, M. (1991). Improved methods for binding protein models in electron density maps and the location of errors in these models. Acta Crystallogr. *A47*, 110–119.
35. Brunger, A.T., et al., and Warren, G.L. (1998). Crystallography & NMR system: A new software suite for macromolecular structure determination. Acta Crystallogr. *D54*, 905–921.
36. Otwinowski, Z., and Minor, W. (1996). Processing of X-ray diffraction data collected in oscillation mode. Methods Enzymol. *276*, 307–326.

Accession Numbers

Atomic coordinates have been deposited in the Protein Data Bank with the accession code 1F5S.